construction materials

MDPI

Article

Thermophysical Properties of Sawdust and Coconut Coir Dust Incorporated Unfired Clay Blocks

Nusrat Jannat [1,2,*], Jeff Cullen [1], Badr Abdullah [1], Rafal Latif Al-Mufti [1] and Karyono Karyono [1,3]

[1] School of Civil Engineering & Built Environment, Liverpool John Moores University, Byrom Street, Liverpool L3 3AF, UK
[2] Department of Architecture, Chittagong University of Engineering & Technology, Chattogram 4349, Bangladesh
[3] Faculty of Engineering and Informatics, Universitas Multimedia Nusantara, Scientia Garden, Gading Serpong, Tangerang 15810, Indonesia
* Correspondence: n.jannat@2019.ljmu.ac.uk

Abstract: Sawdust and coconut coir dust are agro-wastes/by-products which are suitable for use as raw materials to manufacture unfired clay blocks due to their excellent physical and mechanical properties. A limited number of studies have been conducted on the utilisation of these agro-wastes in clay block production, and they have mostly been devoted to investigating the physicomechanical properties, with less attention given to the thermal properties. Moreover, the majority of the studies have used chemical binders (cement and lime) in combination with agro-waste, thus increasing the carbon footprint and embodied energy of the samples. Furthermore, no research has been performed on the thermal performance of these agro-wastes when incorporated into clay blocks at the wall scale. Therefore, to address these limitations, the present study developed unfired clay blocks incorporating sawdust and coconut coir dust (0, 2.5, 5, and 7.5% by weight), without the use of chemical binders, and evaluated their thermal performance, both at the individual and wall scales. The experiments were divided into two phases. In the first phase, individual sample blocks was tested for basic thermal properties. Based on the results of the first phase, small walls with dimensions of 310 mm × 215 mm × 100 mm were built in the second phase, using the best performing mixture from each waste type, and these were assessed for thermal performance using an adapted hot box method. The thermal performance of the walls was evaluated by measuring the heat transfer rate from hot to cold environments and comparing the results to the reference wall. The results showed that thermal conductivity decreased from 0.36 W/mK for the reference sample, to 0.19 W/mK for the 7.5% coconut coir dust sample, and 0.21 W/mK for the 7.5% sawdust sample, indicating an improvement in thermal insulation. Furthermore, the coconut coir dust and sawdust sample walls showed a thermal resistance improvement of around 48% and 35%, respectively, over the reference sample wall. Consequently, the findings of this study will provide additional essential information that will help in assessing the prospective applications of sawdust and coconut coir dust as the insulating material for manufacturing unfired clay blocks.

Keywords: agro-wastes; clay blocks; thermal; unfired; wall

Citation: Jannat, N.; Cullen, J.; Abdullah, B.; Latif Al-Mufti, R.; Karyono, K. Thermophysical Properties of Sawdust and Coconut Coir Dust Incorporated Unfired Clay Blocks. *Constr. Mater.* **2022**, *2*, 234–257. https://doi.org/10.3390/constrmater2040016

Received: 25 August 2022
Accepted: 28 September 2022
Published: 8 October 2022

1. Introduction

The tropics survey report [1] states that over half of the world's population will be residing in tropical regions by 2050, resulting in a considerable rise in demand for indoor thermal comfort. The high temperatures and high humidity features of tropical climates necessitate the development of high thermal resistance building technologies to improve thermal comfort in residential housing. Since the Intergovernmental Panel on Climate Change [2] predicts an increase in global mean surface air temperature of +1.3 to +4.5 °C by the end of the twenty-first century, thermal comfort improvement in this

region is now a key concern [3]. Therefore, researchers have been attempting to alleviate the consequences of global warming by developing novel materials to improve thermal comfort and energy savings in tropical dwellings [4–13]. Earth-based materials have been used for building construction for centuries and are still used in most developing countries [14]. The popularity of these materials is attributed to their easy availability, workability, as well as advantageous hygro-thermal properties [15,16]. Earthen construction generally has a massive thickness, which is responsible for its higher thermal inertia. This feature improves the thermal efficiency of buildings in certain climates by lowering heating and cooling energy demands, resulting in lower operating costs [17,18]. However, in addition to the lack of strength and durability, earthen materials require regular maintenance [15,19,20]. Therefore, there has been growing concern in recent decades about addressing these issues in earthen construction, and different types of stabilisers have been employed to enhance the properties of the earthen materials. Among the various stabilisers, calcium-based materials, such as cement and lime, are widely used due to their easy adaptability and robustness [21,22]. Though such conventional chemical stabilisers can improve several properties of earthen materials, they have certain drawbacks, such as high CO_2 emissions, energy consumption, and cost [23]. Consequently, the development of new stabilisers for earthen material construction with lower environmental impact and processing costs seems to be of great interest among researchers.

The statistics reveal that global agro-waste generation is around 998 million tonnes each year [24,25], and the processing of these wastes is a major issue in developing countries, as most of these wastes are dumped in landfills or burned, which causes serious environmental pollution [26,27]. A number of studies have presented that agro-wastes can be transformed into low-energy and sustainable construction materials, solving a major problem in waste management [28,29]. Sawdust and coconut coir are agro-wastes/by-products which are abundant in tropical countries [30–32]. According to several studies [32–35], these agro-wastes can be used as raw materials in the construction industry due to their excellent physical and mechanical properties. However, a limited number of studies have been carried out using these two agro-wastes in the production of unfired bricks. Khedari et al. [36], Thanushan et al. [37], and Thanushan and Sathiparan [38] produced soil-cement blocks utilising coconut coir fibre and reported that bulk density and compressive strength decreased with the increase in fibre percentage. Moreover, fibre inclusion resulted in a decrease in thermal conductivity [36] and an increase in water absorption rate [38]. On the other hand, the study by Danso et al. [39] revealed that the incorporation of coconut coir fibre into soil blocks remarkably improved mechanical strength and durability. Additionally, the study showed that higher fibre content decreased the linear shrinkage and density, but increased the water absorption rate of the blocks. Sangma et al. [40] assessed the physicomechanical properties of the unfired earth blocks by varying the coconut coir fibre length from 20 mm to 80 mm. The test results demonstrated that the compressive and tensile strength of the samples improved when the fibre length was increased up to 40 mm. Purnomo and Arini [41] developed unfired bricks using lime in combination with treated coconut coir fibre and examined their physicomechanical properties under various humidity conditions. It was observed that better properties were achieved in a high humid environment. Demir [42], Ouattara et al. [43], Vilane [44], and Jokhio et al. [45] investigated the compressive strength of sawdust-incorporated unfired clay bricks and found that the presence of sawdust enhanced the compressive strength. However, according to Ganga et al. [46], Tatane et al. [47], and De Castrillo et al. [48], the compressive strength of the samples decreased with the addition of sawdust. Furthermore, the density and thermal conductivity of the samples declined, whereas capillary water absorption increased with increasing sawdust content [47,48]. Charai et al. [49] also studied the thermal properties of sawdust–clay composites and concluded that sawdust had a positive effect on improving the thermal properties of the samples. The findings of previous studies show that sawdust and coconut coir have the potential to enhance the characteristics of earthen materials.

Research Significance

The literature review presented in the previous section reveals that most of the studies have focused mainly on the investigation of the physicomechanical properties, and limited research is available regarding thermal properties tests. Moreover, the majority of the studies have used chemical binders, such as cement and lime, with agro-wastes to produce the samples. These chemical binders are responsible for environmental degradation, with a high carbon footprint and embodied energy [50]. Hence, the production of agro-wastes incorporated into unfired earth blocks without these binders provides the greatest advantages in terms of sustainability. This study, therefore, investigated the thermophysical properties of the sawdust- and coconut coir dust-blended unfired earth blocks, without any chemical binders.

The literature also shows that studies which measured the thermal properties of the sawdust- and coconut coir dust-incorporated brick are at the individual sample scale. No research has been performed on the thermal performance of these agro-wastes-incorporated clay blocks at the wall scale. The examination of heat transfer rates through building wall materials is important for determining building energy efficiency. Consequently, this study not only measured the thermal properties of individual samples, but also evaluated the thermal performance of the constructed walls in the laboratory using an adapted hot box method. Finally, the test results were compared to the reference sample to reach a conclusion.

The outcomes of this study will support the assessment of the potential application of sawdust and coconut coir dust as insulating materials in the manufacturing of unfired clay blocks.

2. Materials and Methods

2.1. Materials

The materials used to produce the samples were red clay, coconut coir dust, sawdust, and tap water. Square mesh sieves were used to sieve the raw materials to obtain particle sizes between 2 mm–1.18 mm, 1.18 mm–300 µm, and 600 µm–425 µm for red clay, coconut coir dust, and sawdust, respectively (Figure 1). The maximum dry density (2320 kg/m^3) and optimum moisture content (15.50%) of the clay were determined by the standard Proctor compaction test [51], while the Atterberg limit (liquid limit: 31.61%, plastic limit: 19.25, plasticity index: 12.36%) was established following the BS 1377-2:1990 standard [52]. Scanning electron microscopy (SEM) with a conductive coating was used to study the morphology of the raw materials. Moreover, X-ray fluorescence (XRF) and X-ray diffraction (XRD) analysis were used, respectively, for the evaluation of chemical composition and mineralogical phases of raw materials. Furthermore, the thermal characteristics of the raw materials were determined by ISOMET 2114 equipment using a needle probe (Figure 2). The thermophysical properties and chemical compositions of the raw materials are given in Tables 1 and 2, respectively. SEM micrographs revealed that sawdust particles vary in size and form, with heterogeneous fibres and rough surfaces (Figure 3b). On the other hand, the spongy structure of coconut coir dust particles contains numerous pores (Figure 3c). The XRD analysis showed that red clay mainly contains quartz (SiO_2), kaolinite ($Al_2(Si_2O_5)(OH)_4$), and haematite (Fe_2O_3) (Figure 4a), which was also supported by the XRF results presented in Table 2. Coconut coir dust and sawdust were amorphous in form, as observed by the disordered XRD patterns (Figure 4b).

Table 1. Thermophysical properties of raw materials.

Properties	Red Clay	Sawdust	Coconut Coir Dust
Density (kg/m^3)	1430	230	130
Specific gravity	2.32	1.14	0.61
Thermal conductivity (W/mK)	0.30	0.06	0.05

Table 1. *Cont.*

Properties	Red Clay	Sawdust	Coconut Coir Dust
Volumetric heat capacity ($\times 10^6$ J/m^{3}K)	1.29	0.24	0.21
Specific heat capacity (J/kgK)	902.80	1040.43	1583.08
Porosity	0.38	5.09	7.65
Natural moisture content (%)	6.47	5.02	5.62
Water absorption after 24 h under water (%)	27.57	127.66	195.16
Colour	Red	Light brown	Brown

(**a**) (**b**) (**c**)

Figure 1. Photographs of raw materials: (**a**) red clay; (**b**) sawdust; (**c**) coconut coir dust.

Figure 2. Thermal conductivity measurement of raw materials.

Table 2. XRF analysis of the raw materials.

Elements	Weight (%)		
	Red Clay	Sawdust	Coconut Coir Dust
SiO_2	41.454	0.348	4.059
Al_2O_3	15.214	0.390	1.206
K_2O	1.636	0.340	3.942
MgO	5.114	0.408	0.767
Fe_2O_3	8.104	0.186	1.184
Na_2O	1.027	0.926	1.183

Table 2. *Cont.*

Elements	Weight (%)		
	Red Clay	**Sawdust**	**Coconut Coir Dust**
TiO_2	1.411	0.171	0.596
CaO	0.633	1.681	2.782
SO_3	0.047	0.049	0.275
BaO	0.216	0.074	0.089
MnO	0.040	0.026	0.013
ZrO_2	0.035	0.002	0.011
P_2O_5	0.250	0.021	0.094
SrO	0.011	0.000	0.005
CuO	0.006	0.003	0.002
ZnO	0.007	0.004	0.006
Y_2O_3	0.006	0.001	0.001
F	0.050	0.050	0.050
Cl	0.040	0.040	0.040
Co_2O_3	0.007	0.002	0.001
Rb_2O	0.004	-	-
NiO	0.003	-	-
BaO	0.097	-	-
Cr_2O_3	0.016	-	-
Br	-	-	0.001
CHO	24.572	95.278	83.693

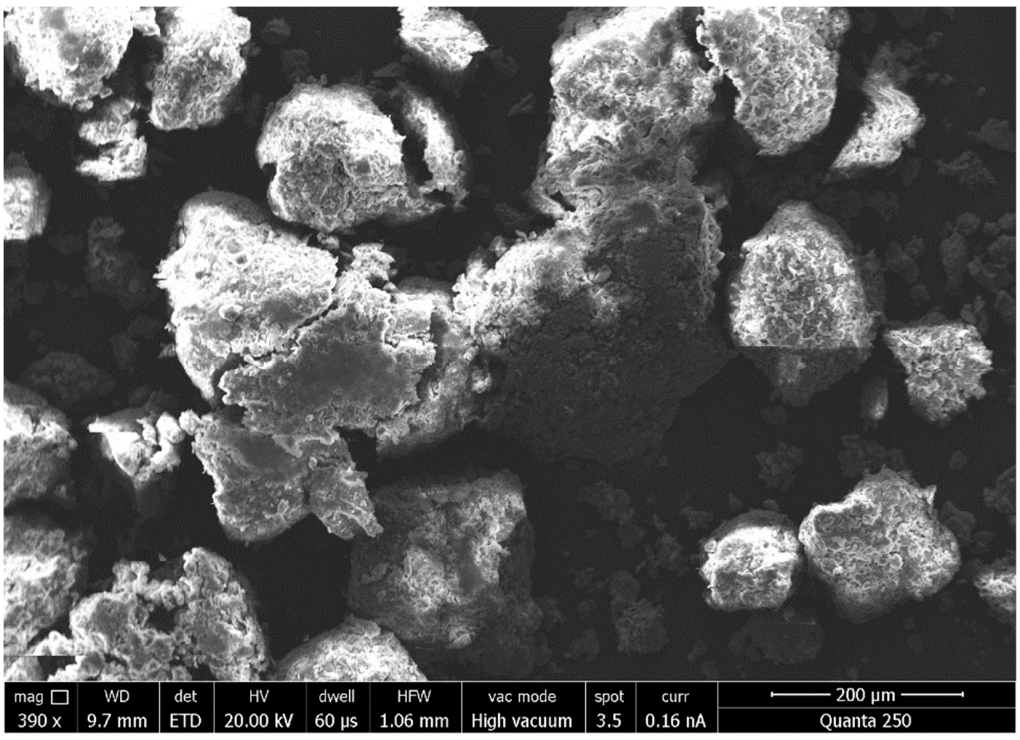

(**a**)

Figure 3. *Cont.*

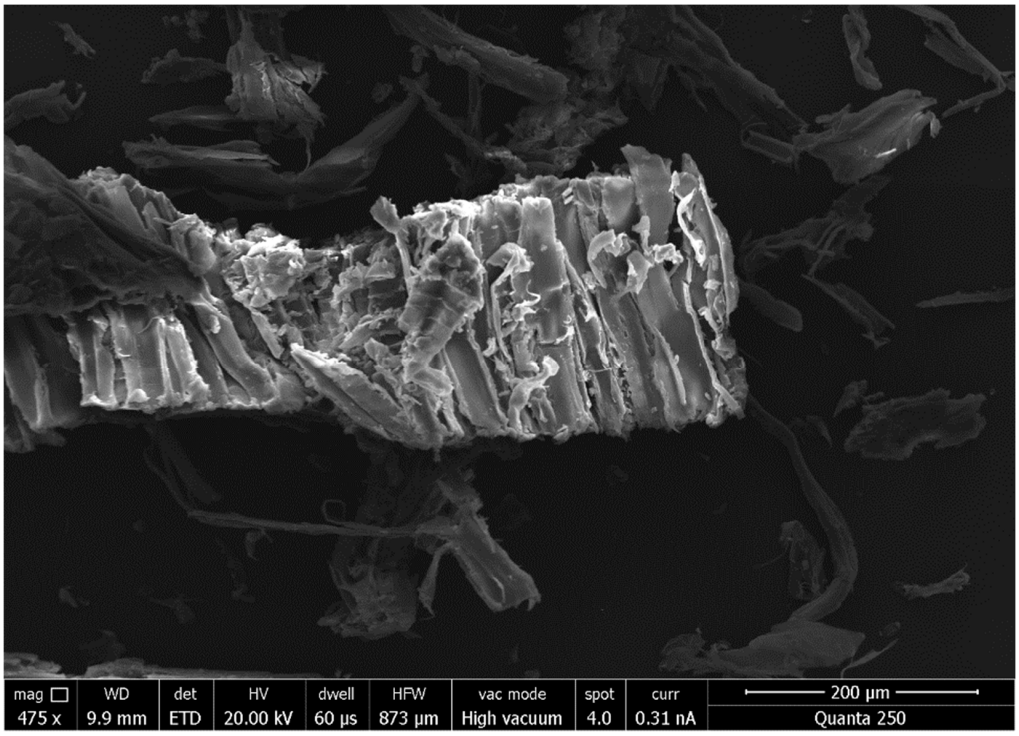

(**b**)

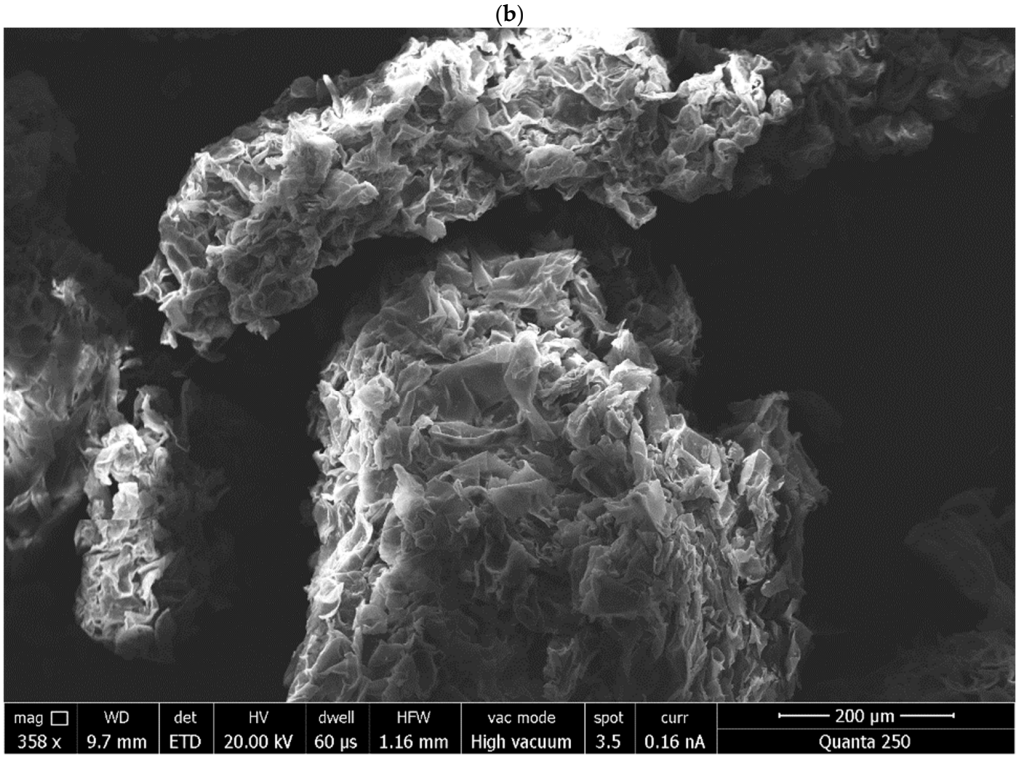

(**c**)

Figure 3. SEM micrographs of raw materials: (**a**) red clay; (**b**) sawdust; (**c**) coconut coir dust.

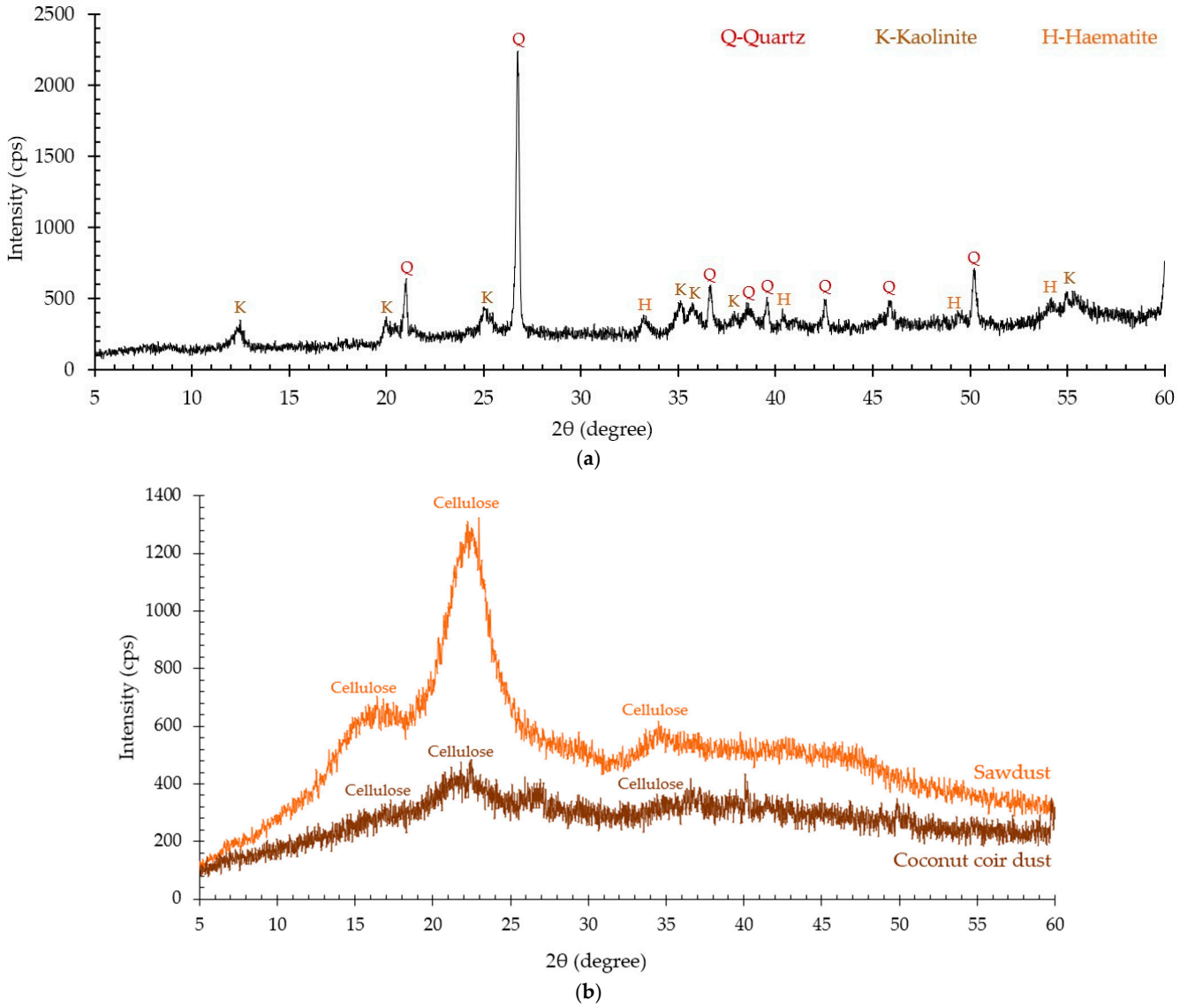

Figure 4. XRD spectra of raw materials: (**a**) red clay; (**b**) sawdust and coconut coir dust.

In this study, sample preparation was executed by hand compaction, since most earthen material building projects in practice employ manual compaction. Table 3 lists the proportions in which the waste materials were added to the clay during sample preparation. The reference case consisted of the sample without waste material. First, dry clay and waste material were thoroughly combined using a mechanical mixer. Then, normal tap water was added and the mixture was blended until it became homogeneous. The proportion of water was adjusted for each series of the mixture to retain the same consistency for moulding. The standardised mould sizes of 100 mm × 100 mm × 100 mm and 100 mm × 100 mm × 215 mm were used for casting the samples. The wet mixture was poured into the mould in two equal layers, and manual compaction was conducted using a square flat section steel rod with 25 blows. A plastic membrane was used to cover the samples for 24 h to avoid rapid loss of moisture. The samples were kept in the moulds for 7 days at a room temperature of 23 °C to 26 °C and a relative humidity of 30% to 34% achieve firmness suitable for demoulding. Before the tests, the demoulded samples were stored for another 21 days in the same environment to dry naturally.

Table 3. Mix composition.

Mix Designation of Samples	Red Clay (g)	Waste (%)		Waste (g)	
		Sawdust	Coconut Coir Dust	Sawdust	Coconut Coir Dust
R	550	0	0	0	0
S-2.5	550	2.5	0	13.75	0
S-5	550	5	0	27.50	0
S-7.5	550	7.5	0	41.25	0
C-2.5	550	0	2.5	0	13.75
C-5	550	0	5	0	27.50
C-7.5	550	0	7.5	0	41.25

2.2. Testing Methods

2.2.1. Thermophysical Properties of Individual Samples

The density of the samples was determined from the mass and volume of the samples according to BS EN 771-1 [53] using the following Equation (1):

$$\rho = M/V \tag{1}$$

where ρ (kg/m^3) is the density, V is the volume (m^3), and M (kg) is the mass of the samples.

The thermal properties (thermal conductivity and volumetric heat capacity) of each mixture were measured using a portable apparatus, ISOMET 2114 model, that directly measures the value via a surface probe attached to a temperature sensor (Figure 5). The experiment was conducted in a laboratory room environment with a temperature of 25 $\pm$ 1 °C and a relative humidity of 32 $\pm$ 2%. Prior to the test, each sample was cleaned with a cloth to remove dust or any interferents. During the experiment, the samples were positioned on a polyurethane block of 50 mm thickness to avoid any potential interference from the adjacent apparatus. For each mix design, two measurements were taken, and the mean was calculated. Knowing the volumetric heat capacity and density of the sample, specific heat capacity was calculated by dividing the volumetric heat capacity by the density value. Furthermore, thermal diffusivity and thermal effusivity were determined by the following Equations (2) and (3) [54]:

$$\alpha = \lambda/\rho C_p \tag{2}$$

$$\tau = \sqrt{\lambda \rho C_p} \tag{3}$$

where α (m^2/s) is the thermal diffusivity, τ (Ws$^{1/2}$/m^{2}K) is the thermal effusivity, λ (W/mK) is the thermal conductivity, ρ (kg/m^3) is the density, and C_p (J/kgK) is the specific heat capacity.

(**a**) (**b**)

Figure 5. Thermal tests: (**a**) 100 mm × 100 mm × 100 mm sample; (**b**) 100 mm × 100 mm × 215 mm sample.

2.2.2. Thermal Properties of Wall Samples

Based on the thermophysical properties of individual samples, the optimal percentage of each waste was chosen to construct small walls to evaluate thermal transmittance. The walls were constructed using two 100 mm × 100 mm × 215 mm blocks and two 100 mm × 100 mm × 100 mm blocks joined together with earth mortar similar to each sample composition. Each wall had a vertical surface area of around 310 mm × 215 mm and a thickness of 100 mm.

Thermal transmittance, also known as the U-value (W/m^2K), is one of the key parameters used to assess the thermal performance of a building envelope, and it can be determined theoretically or experimentally. The theoretical method for calculating the U-value is described in the BS EN ISO 6946 standard [55]. The results obtained from the theoretical method often differ from the in situ U-values [56–58]. The in situ U-value is widely measured following the heat flow meter method specified in the BS ISO 9869-1 standard [59]. In this method, the U-value is calculated by measuring the heat flux through a wall and the temperature difference between the two surfaces (inside and outside) of the wall, since heat is transferred from the warmer to the colder side when there is a temperature difference between two surfaces of a wall. The standard recommends the minimum duration for the test is three days, if the temperature around the heat flux meter is kept steady, but it should be at least seven days to obtain consistent results. Gaspar et al. [60] showed that temperature differences of more than 19 °C require a 72 h test length for low U-value facades, whereas lower temperature differences necessitate a 144 h test time. However, since the temperatures of the hot and cold boxes are controlled in the laboratory, the test duration can be adapted, considering the temperature stability [61].

This study followed the adapted hot box technique [59] (Figure 6), which is a reliable and accurate method for measuring thermal transmittance in laboratory experiments [62–65]. In this method, heat flux between hot and cold chambers was estimated using heat flux sensors. The hot chamber (800 mm × 600 mm × 650 mm) was made of commercially available 50 mm thick polyisocyanurate insulation boards (PIR, λ = 0.022 W/mK, R = 2.25 m^2K/W), which have a thin aluminium foil covering on both sides to keep them isolated from the outside environment. The λ value of this insulation material is comparable to polystyrene foam (0.035 W/mK) [62], expanded polystyrene (0.034 W/mK) [63], and foam polyurethane (0.0245 W/mK) [66], which were used in previous studies to build the hot chamber. Two thermostatic tubular heaters (DIMPLEX ECOT1FT 40 W, 230–240 V) were placed inside the hot chamber as an internal heat source. On the other hand, the cold chamber (450 mm × 600 mm × 750 mm) was a refrigerator used to cool the inside air. The temperatures of the hot and cold chambers were controlled by the EMKO ESM-3711-H temperature controller. The sample wall was positioned between the hot and cold chambers in a sample holder made of double insulation boards (100 mm). Additionally, any gaps between the wall and the sample holder were filled with insulation material (polyisocyanurate insula-

tion, $\lambda = 0.022$ W/mK, R = 2.25 m^2K/W) and then sealed with aluminium foil tape to ensure that heat propagation could only occur through the exposed wall surfaces. Furthermore, inside both chambers, a small fan was placed to prevent any thermal stratification and to ensure uniform heating and cooling [63].

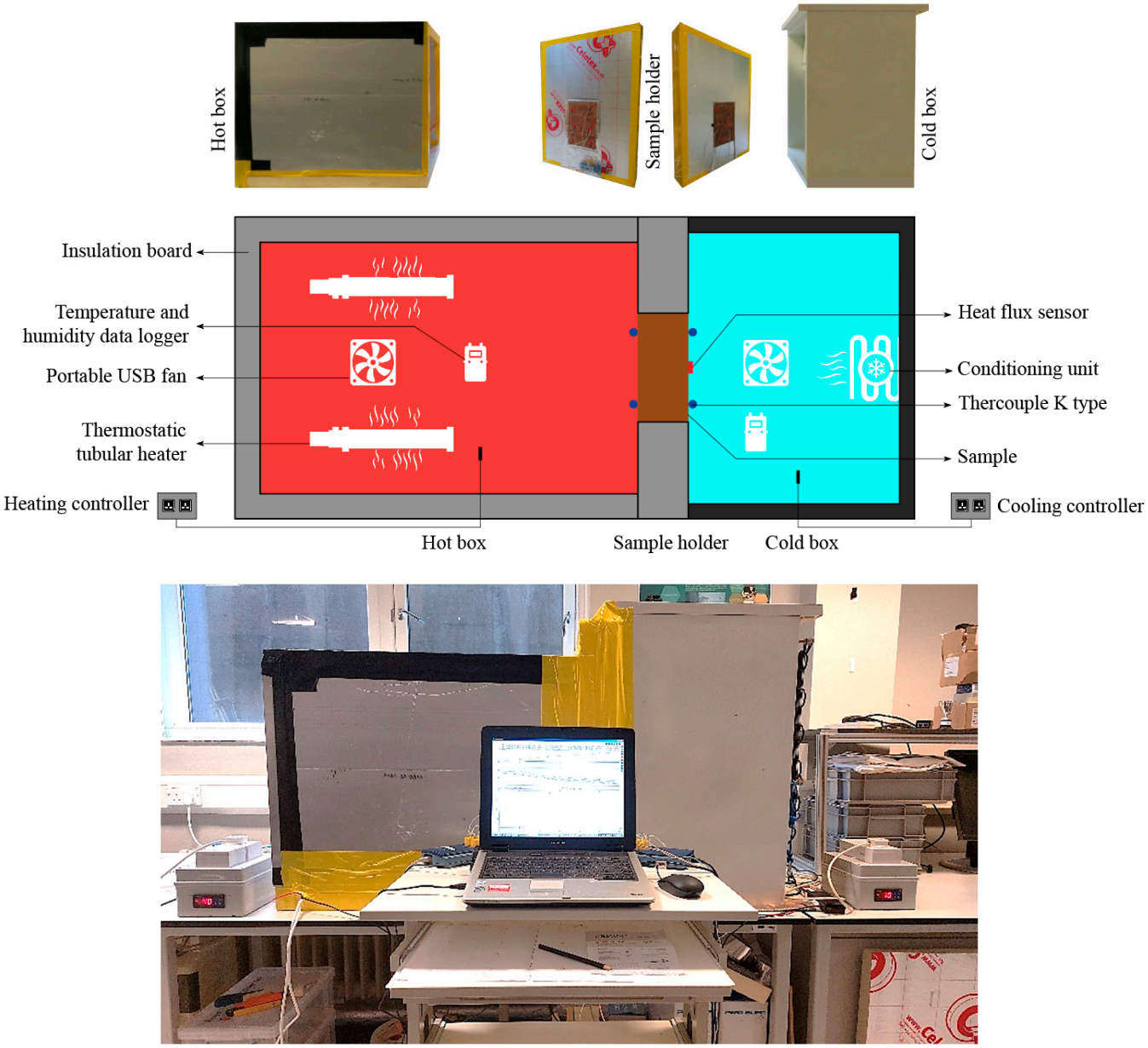

Figure 6. Test setup of thermal transmittance measurement.

The surface temperature of the sample wall was measured using thermocouple K-type sensors attached to the sample wall. On either side of each block of the sample wall, two thermocouple K sensors were installed. In addition, two heat-flux sensors (gSKIN-XB 26 9C) were installed on the sample wall facing the cold room (Figure 7). In order to prevent any influence of air gaps, sandpaper was used to smooth the wall surfaces where the sensors were installed, and adhesive tape was used to fix the sensors to the wall, ensuring that all sensors had good thermal contact with the wall surface. All the sensors were connected to a data logger (Pico USB TC-08) to record the continuous readings for 3 days (72 h), with a sampling period of 5 min. A temperature and relative humidity data logger was also

installed inside both chambers to monitor the temperature and relative humidity of the chambers. Table 4 lists the main materials and equipment used in this experiment.

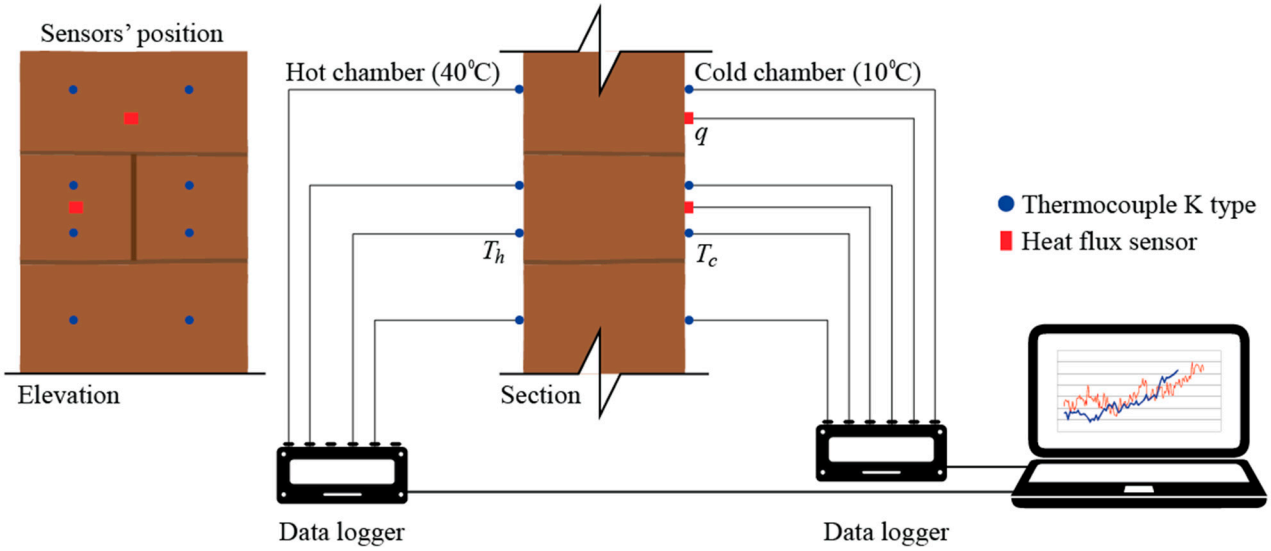

Figure 7. Configuration of the sample wall and position of the sensors.

Table 4. Equipment used for thermal transmittance test setup and measurement.

Equipment	Model	Parameters	Values
Temperature sensor	K-type thermocouple	Accuracy (°C)	±1.5
Heat flux sensor	gSKIN-XB 26 9C	Range (kW/m^2)	−150 to +150
		Sensitivity [μV/(W/m^2)]	1.5
		Calibration accuracy (%)	±3
		Resolution (W/m^2)	0.41
Temperature controller	EMKO ESM-3711-H	Accuracy (%)	±1
Data logger	Pico USB TC-08	Voltage input range (mV)	±70
		Temperature range (°C)	−270 to +1820
		Temperature accuracy (°C)	Sum of ±0.2% of reading and ±0.5
		Voltage accuracy (μV)	Sum of ±0.2% of reading and ±10
Temperature and relative humidity data logger	EL-USB-2 RH/TEMP	Temperature range (°C)	−35 to +80
		Relative humidity range (%)	0 to 100
		Temperature accuracy (°C)	±0.5
		Relative humidity accuracy (%)	±2.25
Heating source	DIMPLEX ECOT1FT thermostatic tubular heater	Heat output (W)	40
		Capacity (V)	230–240
Fan	4″ portable USB fan	Capacity (V)	5

BS ISO 9869-1-2014 [59] specifies the average progressive method to determine the U-value in steady-state conditions. This method is popular, since it simplifies the calculating procedure, despite the longer test period. The reliability of this method depends on the temperature difference between the two chambers. The higher the temperature difference, the more reliable the results. Meng et al. [67] revealed that raising the temperature difference on both sides of walls reduces the maximum system error (measurement error) and recommended maintaining a temperature difference of over 20 °C on both sides of the wall

to decrease the maximum system error. Hence, in this study, throughout the test period, the average air temperatures of the hot and cold chambers were maintained at 40 °C and 10 °C, respectively. The heat flux was measured at two locations on the sample wall over a period of at least 3 days (72 h), fulfilling the minimum duration requirement stipulated by the standard. Using Equation (4) from the standard, the U-value of the sample wall was derived by dividing the heat flux data through the wall by the temperature difference between the two surfaces (hot and cold) of the wall.

$$U = \frac{q}{(T_h - T_c)} \quad (4)$$

where q is the density of heat flow rate (W/m^2), T_h is the hot side temperature (°C), and T_c is the cold side temperature (°C) of the sample.

The thermal resistance or R-value (m^{2}K/W) of the wall can be obtained by inverting the total thermal transmittance determined (R = 1/U).

3. Results and Discussions

3.1. Thermophysical Properties of Individual Samples

Table 5 presents the results of the thermophysical properties of different agro-waste-blended samples. As shown in the table, the bulk density decreased as the waste content increased. Similar results were observed in several previous studies, where the inclusion of natural fibres or aggregates into the formulation of unfired earthen blocks resulted in a gradual decrease in bulk density [68–70]. This can be explained by the fact that when comparatively lighter sawdust and coconut coir dust particles (see Table 1) were incorporated into the mixture, they displaced the heavier clay particles, which eventually decreased the density. Moreover, during sample preparation, the hydrophilic sawdust and coconut coir dust (see water absorption values in Table 1) swelled by absorbing water. After drying, they returned almost to their former size, leaving very small air voids between their outer periphery and the clay particles. Consequently, the more sawdust and coconut coir dust were added to the mixture, the more air voids were created [71]. The samples with sawdust had densities ranging from 1837.05 kg/m^3 to 1638.64 kg/m^3 for 2.5% to 7.5% content, while for the same coconut coir dust content, the density declined from 1725.44 kg/m^3 to 1552.52 kg/m^3 corresponding to a decrease of up to 22% and 26%, respectively, for sawdust and coconut coir dust in comparison to the waste-free clay sample.

Table 5. Average values and coefficient of variation (% in parenthesis) of thermophysical properties of the sample blocks.

Sample ID	Density, ρ (kg/m^3)	Thermal Conductivity, λ (W/mK)	Volumetric Heat Capacity, ρC_p ($\times 10^6$ J/m^{3}K)	Specific Heat Capacity, C_p (J/kgK)	Thermal Diffusivity, α ($\times 10^{-6}$ m^2/s)	Thermal Effusivity, τ (Ws$^{1/2}$/m^{2}K)
R	2090.96 ± 2.55 (0.32)	0.36 ± 0.02 (0.14)	1.66 ± 0.25 (0.33)	794.75	0.217	774.70
S-2.5	1837.05 ± 2.36 (0.08)	0.26 ± 0.01 (0.22)	1.51 ± 0.23 (0.31)	824.12	0.173	629.44
S-5	1735.85 ± 2.35 (0.13)	0.24 ± 0.01 (0.30)	1.47 ± 0.22 (0.33)	849.41	0.161	591.14
S-7.5	1638.64 ± 2.34 (0.09)	0.21 ± 0.01 (0.41)	1.42 ± 0.21 (0.43)	865.39	0.145	539.96
C-2.5	1725.44 ± 2.54 (0.24)	0.25 ± 0.01 (0.23)	1.46 ± 0.22 (0.41)	848.68	0.168	600.19
C-5	1638.79 ± 2.56 (0.25)	0.22 ± 0.01 (0.32)	1.41 ± 0.21 (0.39)	859.45	0.159	561.19
C-7.5	1552.52 ± 2.59 (0.27)	0.19 ± 0.01 (0.47)	1.38 ± 0.21 (0.47)	886.20	0.142	517.77

The thermal conductivity of building materials is an important factor for evaluating thermal performance, since it has a direct influence on heat losses and energy consumption in the building [72–74]. The thermal conductivity of a material is affected by various

variables, including its morphology, density, and homogeneity [75,76]. The results in Table 5 indicate a gradual decrease in thermal conductivity values with the increase in waste percentages. This drop can be attributed to both the lower thermal conductivity of the agro-waste materials employed (see Table 1) and an increase in the amount of air in the sample combination. The thermal conductivity of a material is inversely proportional to its porosity [77]. The addition of agro-wastes reduces the density of the samples, resulting in a higher void volume, which is usually filled with air. Due to the low conductivity of air (0.024–0.026 W/mK), the thermal conductivity of the samples decreases as the volume of air in the void increases [78–80].

In Figure 8, the thermal conductivity values of the samples tested are plotted against their density. There is a linear connection between sample density and thermal conductivity, with lower density samples having lower thermal conductivity than higher density samples. The findings are consistent with the conclusions reached in previous investigations [68,72,81,82]. Moreover, the microscopic examination of the raw materials (Figure 3) revealed that sawdust and coconut coir dust particles exhibited cellular porous structures that may contain air, explaining their low thermal conductivity values. Furthermore, it appears that the use of coconut coir dust leads to marginally better insulation (i.e., lower thermal conductivity values) than sawdust. This may be due to the lower bulk density and spongy structure of coconut coir dust particles, containing more air voids than sawdust. The lowest thermal conductivity values for the coconut coir dust and sawdust samples was achieved at a 7.5% content, which was about a 46% and 43% decrease compared to the reference sample.

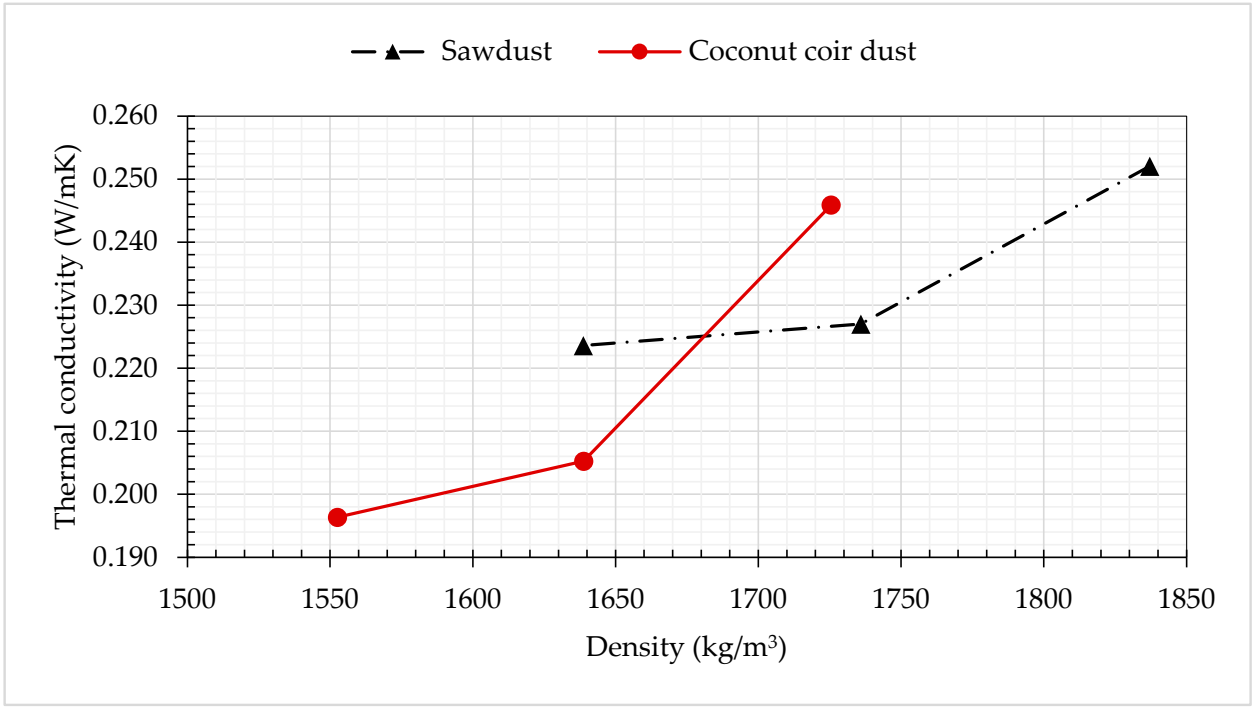

Figure 8. Correlation between thermal conductivity and density.

The volumetric heat capacity of the agro-waste-incorporated samples dropped because of the considerable decrease in the samples' density (see Table 5). However, the specific heat capacity of the samples increased with the increasing waste percentage, since the agro-wastes, which have a lower mass content than clay, had greater specific heat capacity values [68]. The experimental results revealed that a 7.5% coconut coir dust and 7.5% sawdust addition raised the specific heat capacity from 848.68 J/kgK to 886.20 J/kgK and 824.12 J/kgK to 865.39 J/kgK, resulting in an increase of about 12% and 9%, respectively, over the reference sample. Moreover, the coconut coir dust samples had a slightly higher

specific heat capacity than the sawdust samples. The higher porosity in coconut coir dust samples than in sawdust samples might be responsible for this, as the pores are primarily filled with air, which has a specific heat capacity of 1005 J/kgK [83].

The thermal inertia of buildings contributes to both thermal comfort and a reduction in energy consumption by keeping the indoor air temperature stable. There are two forms of inertia: transmission and absorption. Transmission inertia is defined by thermal diffusivity, whereas absorption inertia is described by thermal effusivity. In buildings, materials with low diffusivity and high effusivity should be used to improve thermal inertia [84,85]. In areas where cooling is a major issue, using low thermal diffusivity materials can delay heat transfer from the outside of the building to the inside, decreasing the indoor temperature of the building and reducing the demand for air conditioning during the summer. Materials with high thermal effusivity can also help to keep the indoor temperature of a building stable in the summer by storing and releasing heat. When the internal temperature of a building rises above the comfort level, the walls absorb heat until a steady temperature is attained. This heat is released when the building's internal temperature falls below a comfortable level. Similarly, in the winter, these high effusive materials can also aid in the reduction in heating demand [86,87]. As a result, it is recommended that two distinct materials be used to improve indoor thermal comfort: one with low diffusivity on the exterior side as an insulating material and the other with high effusivity on the interior side of the building wall as a structural material [84].

Table 5 also shows that the thermal diffusivity and thermal effusivity of the samples decreased when the percentage of agro-wastes increased in the mixture. Laborel-Préneron et al. [68] also observed a similar trend in results using hemp shiv, corn cob, and barley straw in unfired earthen bricks. The thermal diffusivity decreased from 0.178×10^{-6} m^2/s to 0.142×10^{-6} m^2/s and 0.173×10^{-6} m^2/s to 0.145×10^{-6} m^2/s, respectively, when the coconut coir dust and sawdust content increased from 0.25% to 7.5%, indicating a positive influence of agro-wastes on dampening the thermal diffusion in the produced clay blocks [88]. It was also found that the thermal effusivity values declined from 600.19 $Ws^{1/2}/m^2K$ to 517.77 $Ws^{1/2}/m^2K$ and 629.44 $Ws^{1/2}/m^2K$ to 539.96 $Ws^{1/2}/m^2K$, respectively, for increasing the same amount of coconut coir dust and sawdust. According to the results, the addition of agro-wastes to the unfired clay block increases the transmission inertia, while decreasing the absorption inertia. These types of materials would be better suited to the construction of exterior walls to delay the transmission of heat from the outside to the inside [68].

3.2. Thermal Properties of Wall Samples

According to the results of the thermophysical properties of the individual samples, the S-7.5 and C-7.5 samples had the lowest density, thermal conductivity, and diffusivity, as well as the highest specific heat capacity values. Hence, the S-7.5 and C-7.5 samples were used to make small walls to evaluate their thermal transmittance and resistance. Instead of collecting data immediately, data was collected for at least 24 h after the system attained a thermal steady-state condition. Thermography analysis was performed on both sides of the walls to check for any irregularities introduced by the heating and cooling sources. According to Figure 9, the wall surface areas are not affected by any probable source of error.

The temperature profiles of the two sides (hot and cold) of the wall surfaces (72 h) are shown in Figure 10. The figure shows that all the walls have nearly similar temperatures on both surfaces, indicating that wall surface temperatures are unaffected by the material properties, which was also confirmed by the experimental results of Bruno et al. [89]. The slight temperature difference is due to the position of the temperature sensors on the surface of the sample block. Despite the sensors being attached as near to the surface as feasible, a gap between the sensor and the surface may be created, leading it to record the temperature of the surrounding air at some point.

Figure 11 illustrates the monitored relative humidity inside the hot and cold chambers during the test period. The recorded average relative humidity during the last 24 h test period in the hot chamber varied between 14.62% and 15.35%, while it varied between 39.09% and 41.29% in the cold chamber.

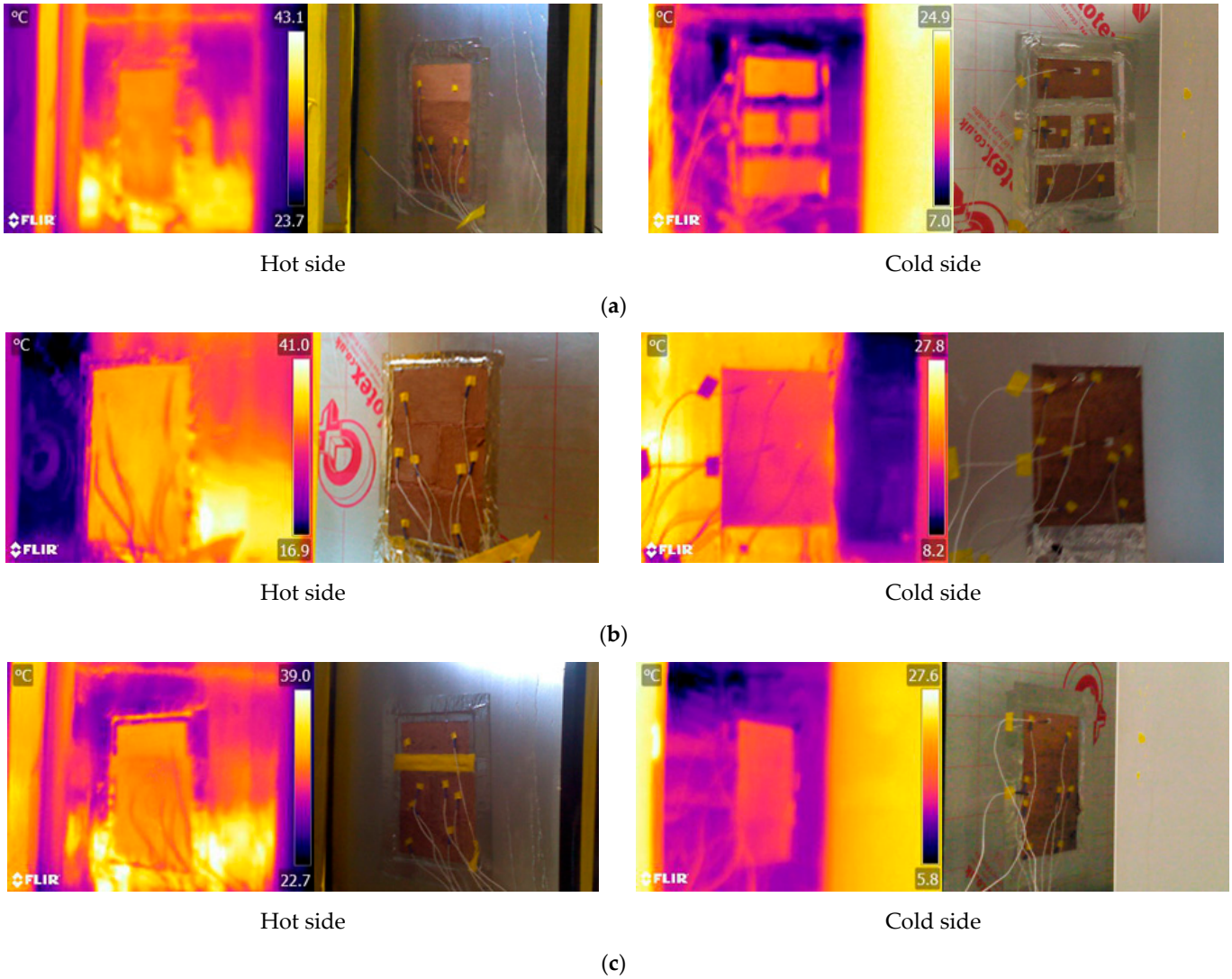

Figure 9. Thermographs of different wall surfaces: (**a**) reference wall; (**b**) sawdust wall; (**c**) coconut coir dust wall.

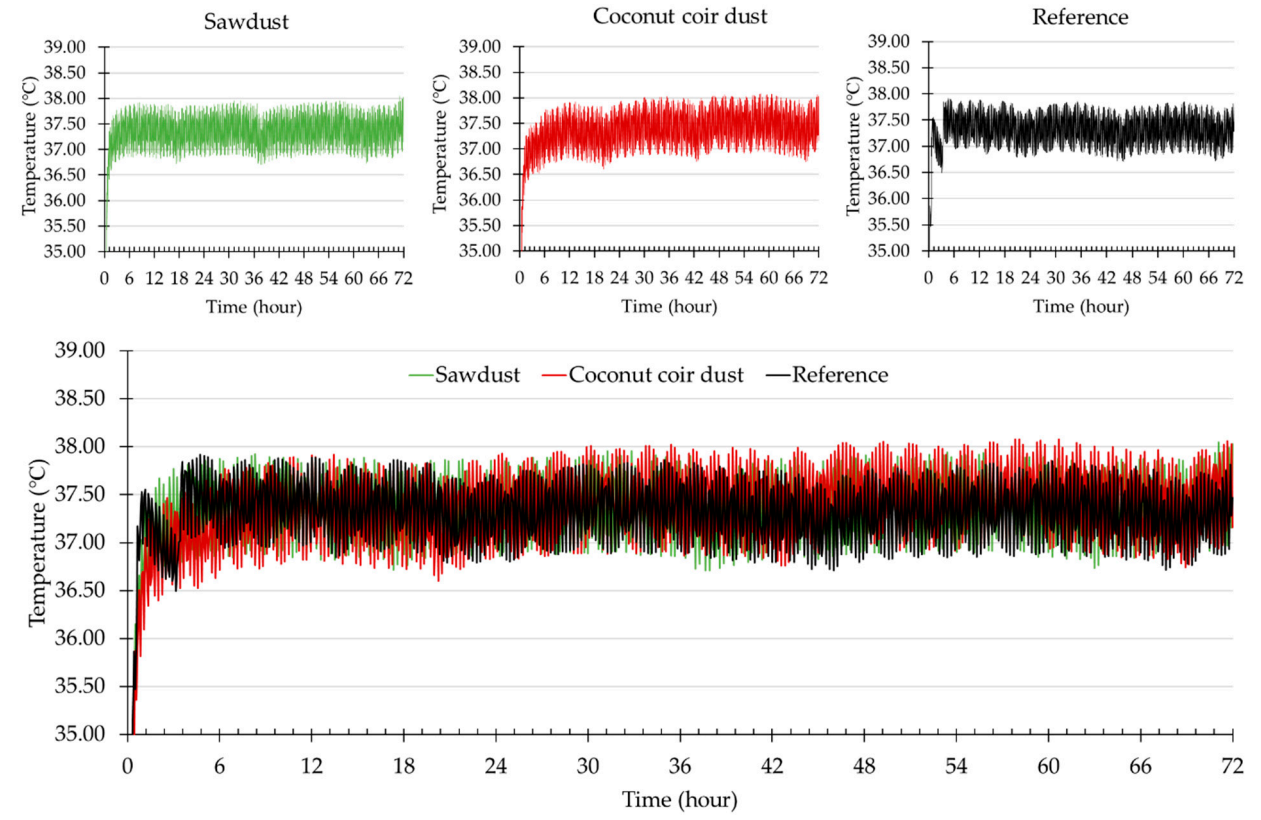

(**a**)

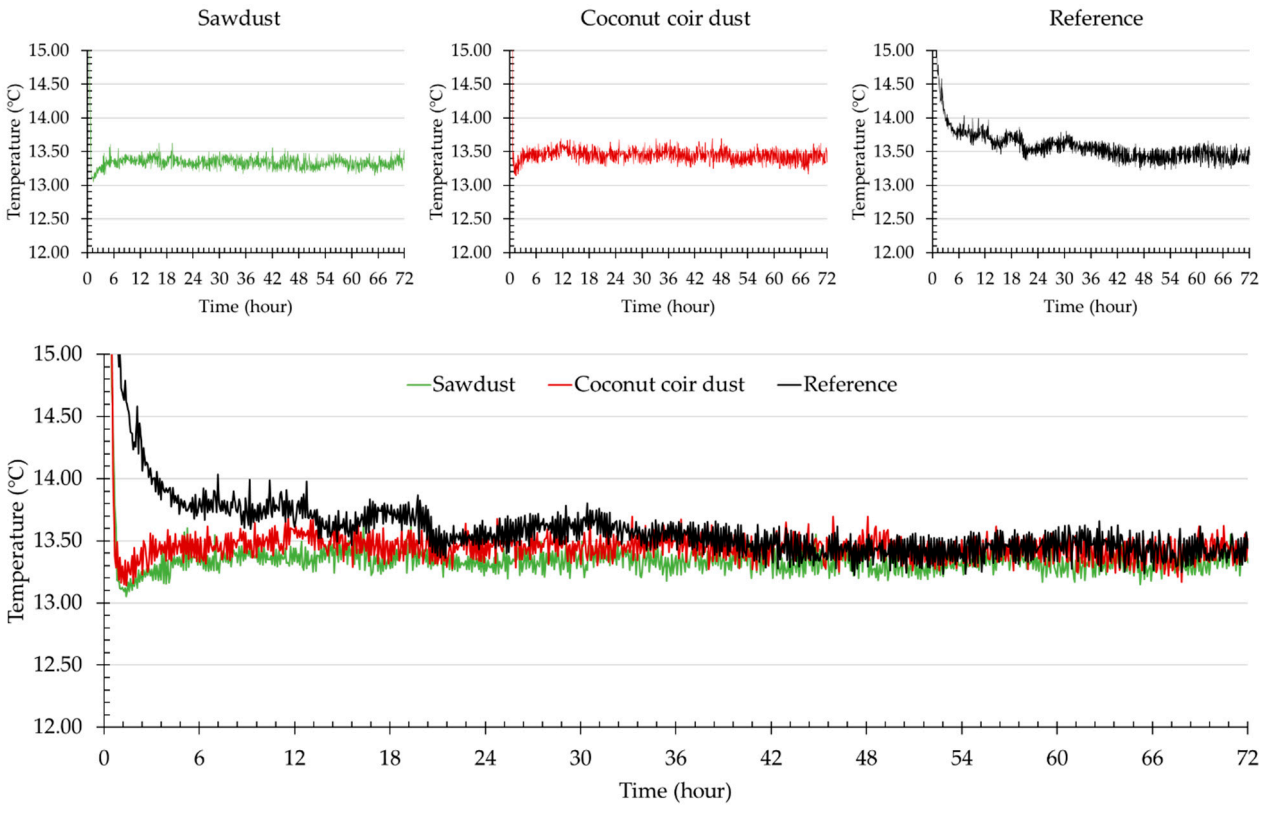

(**b**)

Figure 10. Wall surface temperature profiles (72 h): (**a**) hot side; (**b**) cold side.

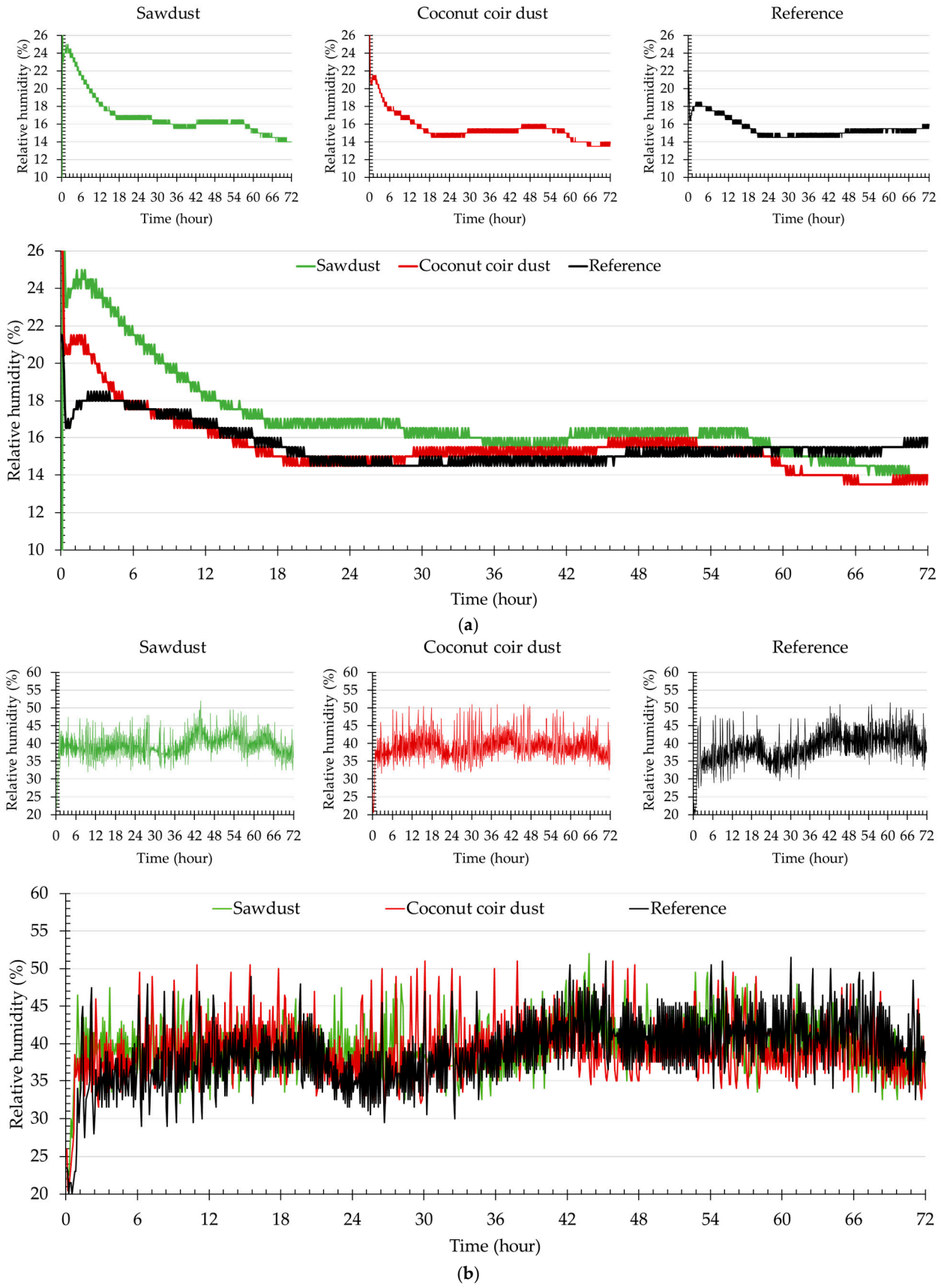

Figure 11. Relative humidity (72 h): (**a**) hot chamber; (**b**) cold chamber.

Table 6 lists the results of the last 24 h of the different wall sample test. The heat flux measured through the walls exhibited a similar pattern (Figure 12), but with different magnitudes. The reference wall had the highest heat flux value of 548.17 W/m^2, followed by the heat flux in the sawdust wall, with a value of 407.53 W/m^2, while the heat flux of the coconut coir dust wall showed the lowest value of 369.96 W/m^2. The lower thermal conductivity and density of the coconut coir dust sample may contribute to the lower heat flux. Materials with a higher thermal transmittance, or U-value, lose more heat, whereas those with a lower U-value lose less heat. The results show that the coconut coir dust sample had the lowest U-value, indicating the highest thermal resistance, as thermal resistance is inversely proportional to the thermal transmittance. The thermal resistance of the coconut coir dust and sawdust sample walls increased by around 48% and 35%, respectively, as compared to the reference sample wall.

Table 6. Average results of last 24 h of the wall test.

	Measurements	**Wall ID**		
		R	**S-7.5**	**C-7.5**
Average values (Last 24 h)	Thickness (mm)	100	100	100
	Surface Temperature (hot side) (°C)	37.32	37.40	36.46
	Surface Temperature (cold side) (°C)	13.44	13.32	13.42
	Temperature Difference (°C)	23.88	23.08	23.04
	Heat Flux (W/m^2)	548.17	407.53	369.96
	U-value (W/m^{2}K)	1.85	1.37	1.24
	R-value (m^{2}K/W)	0.54	0.73	0.80

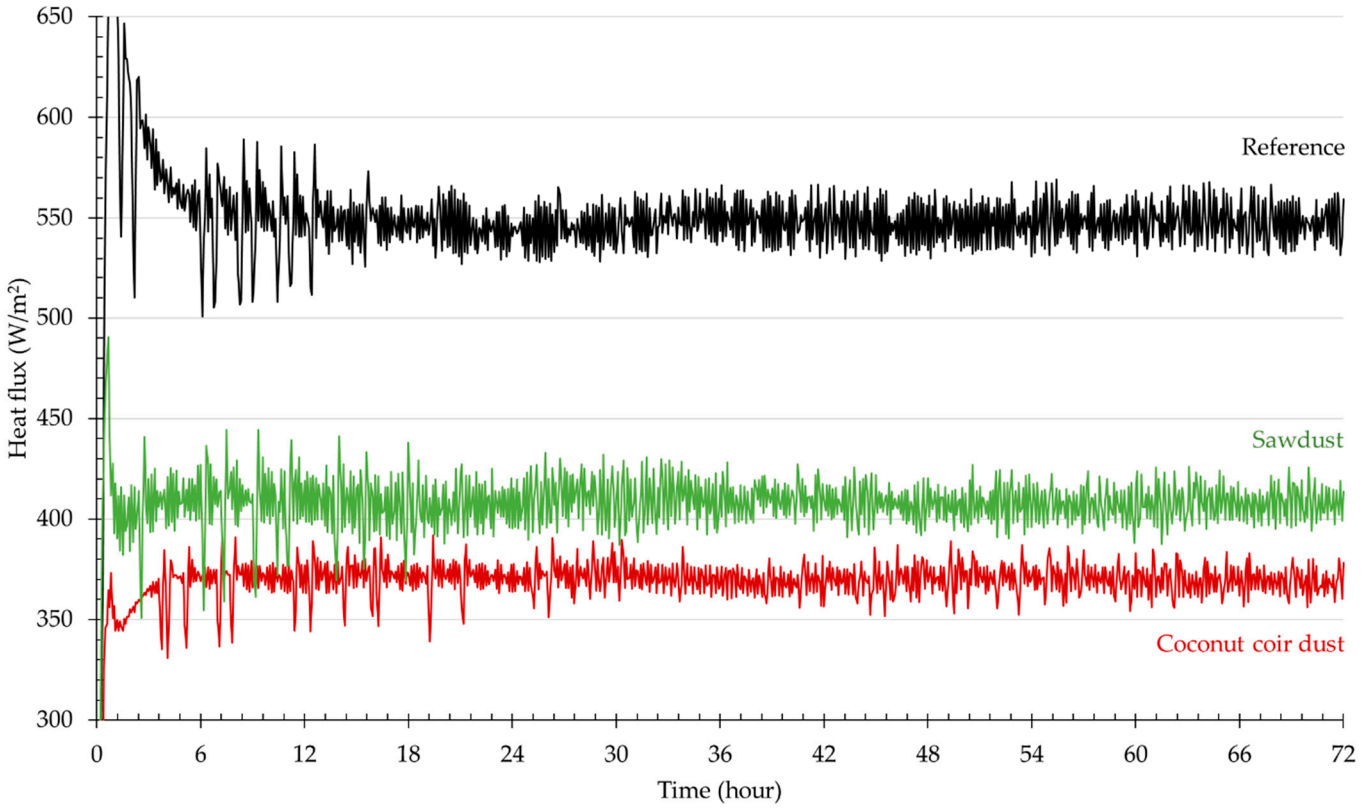

Figure 12. Heat fluxes across the walls (72 h).

In Figure 13, the experimental U-value results of different wall constructions are compared to the findings of several studies in the literature [90–94]. Due to the different thicknesses of the experimented walls and since the U-value is highly dependent on the thickness of the wall, the apparent thermal conductivity values of the walls are calculated by multiplying the U-value by the thickness of the wall to obtain a better comparison of their thermal efficiency [95]. However, it should be noted that the literature thus far reflects very few conducted and published tests.

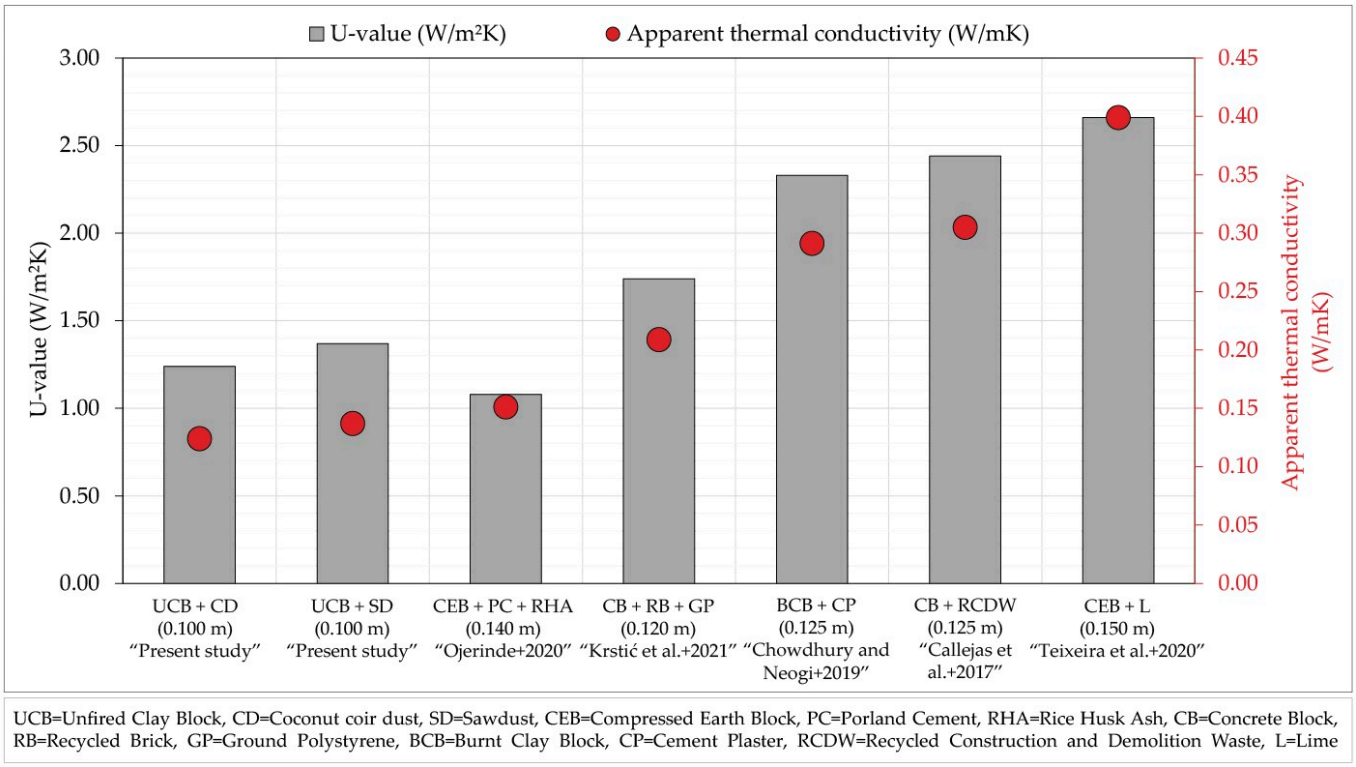

Figure 13. Comparison of U-values of different walls with literature results [90–94].

Ojerinde [90] observed that a 10% to 30% rice husk ash addition as a partial replacement for Portland cement in compressed earth brick production decreased the U-value from 1.076 W/m^{2}K to 1.086 W/m^{2}K. In another study, Teixeira et al. [94] found a U-value of 2.66 W/m^{2}K using 7% lime in the compressed earth brick wall. Krstić et al. [91] used two methods (heat flow and temperature based) to measure the in situ U-value of a hollow concrete masonry block wall made with recycled crushed brick waste and ground polystyrene. According to the study, the U-values for the wall without any insulation ranged from 1.740 W/m^{2}K to 1.782 W/m^{2}K for the heat flow method, while for the temperature based method, the U-value was 1.363 W/m^{2}K. In the case of a burnt clay brick wall with cement plaster, using the guarded hot box method, Chowdhury and Neogi [92] reported that the U-value ranged from 2.326 W/m^{2}K to 2.488 W/m^{2}K. Callejas et al. [93] also used an adapted hot box method to determine the thermal properties of concrete block with recycled construction and demolition waste. Based on the results obtained, the block was found to have a U-value of between 2.439 W/m^{2}K and 3.030 W/m^{2}K in the solid area. After reviewing the experimental results described in the literature, it can be concluded that coconut coir dust and sawdust have great potential for improving the thermal properties of unfired clay brick.

4. Conclusions

This study aimed to experimentally investigate the thermophysical properties of the produced unfired clay blocks utilising sawdust and coconut coir dust wastes. The properties

measured include density, thermal conductivity, volumetric heat capacity, specific heat capacity, thermal diffusivity, and thermal effusivity. Furthermore, the thermal efficiency of the constructed walls with dimensions of 310 mm × 215 mm × 100 mm was evaluated using an adapted hot box method in which two surfaces of the wall were exposed to hot and cold temperatures, and heat flow across the wall was measured concurrently.

The test findings lead to the following conclusions:

- The presence of more waste content in the mixture decreased the density and consequently lowered the thermal conductivity of the samples. Based on the fact that coconut coir dust particles are lighter than sawdust particles, samples reinforced with coconut coir dust provided better thermal insulation than those reinforced with sawdust. When compared to the reference sample, the addition of coconut coir dust and sawdust resulted in a decrease of about 26% and 22% in density, as well as 46% and 43% in thermal conductivity, respectively.
- Moreover, waste inclusion contributed to lowering the volumetric heat capacity, thermal diffusivity, and thermal effusivity, while increasing the specific heat capacity of the samples.
- Furthermore, the wall made of 7.5% coconut coir dust had the best thermal performance, which may be attributed to the lightweight nature of the samples. Lightweight samples contain more air voids, which reduces the amount of heat transfer from hot to cold environments. The coconut coir dust and sawdust sample walls outperformed the reference sample wall in terms of thermal resistance, with an improvement of around 48% and 35%, respectively.
- Considering the thermal performance, it can be concluded that both types of agro-waste incorporation enhanced the overall thermal properties of the produced unfired clay blocks.

The findings of this study will contribute to the literature by adding information related to the thermal performance of agro-wastes incorporated into unfired clay blocks. Moreover, this study will be beneficial for building material manufacturers, as it proposes a methodology for developing environmentally friendly unfired clay blocks. Furthermore, the production of clay blocks with agro-wastes will provide a sustainable solution to the waste disposal problem.

In this study, small walls were tested in the laboratory to determine the thermal characteristics of agro-waste-incorporated unfired clay blocks, in which the findings are not fully conclusive. Therefore, future research might employ in situ performance measurement of the wall materials to arrive at a more realistic conclusion. Future research can also investigate the properties of agro-waste-incorporated clay blocks using different types of clay/soil.

Author Contributions: Methodology, N.J. and J.C.; investigation, N.J., J.C. and K.K.; supervision, B.A. and R.L.A.-M.; writing—original draft, N.J.; writing—review and editing, B.A., R.L.A.-M. and K.K. All authors have read and agreed to the published version of the manuscript.

Funding: This research received no external funding.

Data Availability Statement: Not applicable.

Acknowledgments: The authors gratefully acknowledge the financial and laboratory assistance provided by the School of Civil Engineering and Built Environment at Liverpool John Moores University, United Kingdom.

Conflicts of Interest: The authors declare no conflict of interest.

References

1. Rodriguez, C.M.; D'Alessandro, M. Indoor thermal comfort review: The tropics as the next frontier. *Urban Clim.* **2019**, *29*, 100488. [CrossRef]
2. Stocker, T.F.; Dahe, Q.; Plattner, G.K.; Tignor, M. IPCC workshop on regional climate projections and their use in impacts and risk analysis studies. In *Workshop Report*; Intergovernmental Panel on Climate Change: Bern, Switzerland, 2015; p. 18.

3. Lundgren-Kownacki, K.; Hornyanszky, E.D.; Chu, T.A.; Olsson, J.A.; Becker, P. Challenges of using air conditioning in an increasingly hot climate. *Int. J. Biometeorol.* **2018**, *62*, 401–412. [CrossRef] [PubMed]
4. Latha, P.K.; Darshana, Y.; Venugopal, V. Role of building material in thermal comfort in tropical climates—A review. *J. Build. Eng.* **2015**, *3*, 104–113. [CrossRef]
5. Hashemi, A. Effects of thermal insulation on thermal comfort in low-income tropical housing. *Energy Procedia* **2017**, *134*, 815–824. [CrossRef]
6. Zune, M.; Rodrigues, L.; Gillott, M. Vernacular passive design in Myanmar housing for thermal comfort. *Sustain. Cities Soc.* **2020**, *54*, 101992. [CrossRef]
7. Aflaki, A.; Mahyuddin, N.; Mahmoud, Z.A.C.; Baharum, M.R. A review on natural ventilation applications through building façade components and ventilation openings in tropical climates. *Energy Build.* **2015**, *101*, 153–162. [CrossRef]
8. Tatarestaghi, F.; Ismail, M.A.; Ishak, N.H. A comparative study of passive design features/elements in Malaysia and passive house criteria in the tropics. *J. Des. Built Environ.* **2018**, *18*, 15–25. [CrossRef]
9. Shuhaimi, N.D.A.M.; Zaid, S.M.; Esfandiari, M.; Lou, E.; Mahyuddin, N. The impact of vertical greenery system on building thermal performance in tropical climates. *J. Build. Eng.* **2022**, *45*, 103429. [CrossRef]
10. Emmanuel, R. An analysis of the bio-climatic effects of roof cover of domestic buildings in the equatorial tropics. *Archit. Sci. Rev.* **2002**, *45*, 117–124. [CrossRef]
11. Bimaganbetova, M.; Memon, S.A.; Sheriyev, A. Performance evaluation of phase change materials suitable for cities representing the whole tropical savanna climate region. *Renew. Energy* **2020**, *148*, 402–416. [CrossRef]
12. De Waal, H.B. New recommendations for building in tropical climates. *Build. Environ.* **1993**, *28*, 271–285. [CrossRef]
13. Soubdhan, T.; Feuillard, T.; Bade, F. Experimental evaluation of insulation material in roofing system under tropical climate. *Sol. Energy* **2005**, *79*, 311–320. [CrossRef]
14. Auroville Earth Institute. Building with Earth, Technique Overview. Available online: http://www.earth-auroville.com/world_techniques_introduction_en.php (accessed on 20 May 2022).
15. Adegun, O.B.; Adedeji, Y.M.D. Review of economic and environmental benefits of earthen materials for housing in Africa. *Front. Archit. Res.* **2017**, *6*, 519–528. [CrossRef]
16. Sheweka, S. Using mud bricks as a temporary solution for Gaza reconstruction. *Energy Procedia* **2011**, *6*, 236–240. [CrossRef]
17. El Fgaier, F.; Lafhaj, Z.; Brachelet, F.; Antczak, E.; Chapiseau, C. Thermal performance of unfired clay bricks used in construction in the north of France: Case study. *Case Stud. Constr. Mater.* **2015**, *3*, 102–111. [CrossRef]
18. Elias-Ozkan, S.T.; Summers, F.; Surmeli, N.; Yannas, S. A comparative study of the thermal performance of building materials. In Proceedings of the PLEA2006—The 23rd Conference on Passive and Low Energy Architecture, Geneva, Switzerland, 6–8 September 2006.
19. Araya-Letelier, G.; Concha-Riedel, J.; Antico, F.C.; Sandoval, C. Experimental mechanical-damage assessment of earthen mixes reinforced with micro polypropylene fibers. *Constr. Build. Mater.* **2019**, *198*, 762–776. [CrossRef]
20. Kulshreshtha, Y.; Mota, N.J.A.; Jagadish, K.S.; Bredenoord, J.; Vardon, P.J.; Van Loosdrecht, M.C.M.; Jonkers, H.M. The potential and current status of earthen material for low-cost housing in rural India. *Constr. Build. Mater.* **2020**, *247*, 118615. [CrossRef]
21. Prusinski, J.R.; Bhattacharja, S. Effectiveness of Portland cement and lime in stabilizing clay soils. *Transp. Res. Rec.* **1999**, *1652*, 215–227. [CrossRef]
22. Nagaraj, H.B.; Sravan, M.V.; Arun, T.G.; Jagadish, K.S. Role of lime with cement in long-term strength of Compressed Stabilized Earth Blocks. *Int. J. Sustain. Built Environ.* **2014**, *3*, 54–61. [CrossRef]
23. Ouedraogo, K.A.J.; Aubert, J.E.; Tribout, C.; Escadeillas, G. Is stabilization of earth bricks using low cement or lime contents relevant? *Constr. Build. Mater.* **2020**, *236*, 117578. [CrossRef]
24. Agamuthu, P. Challenges and opportunities in agro-waste management: An Asian perspective. In Proceedings of the Inaugural Meeting of First Regional 3R Forum in Asia, Tokyo, Japan, 11–12 November 2009.
25. Tahir, T.A.; Hamid, F.S. Vermicomposting of two types of coconut wastes employing Eudrilus eugeniae: A comparative study. *Int. J. Recycl. Org. Waste Agric.* **2012**, *1*, 7. [CrossRef]
26. Wang, B.; Dong, F.; Chen, M.; Zhu, J.; Tan, J.; Fu, X.; Wang, Y.; Chen, S. Advances in recycling and utilization of agricultural wastes in China: Based on environmental risk, crucial pathways, influencing factors, policy mechanism. *Procedia Environ. Sci.* **2016**, *31*, 12–17. [CrossRef]
27. Maji, S.; Dwivedi, D.H.; Singh, N.; Kishor, S.; Gond, M. Agricultural waste: Its impact on environment and management approaches. In *Emerging Eco-Friendly Green Technologies for Wastewater Treatment*; Bharagava, R.N., Ed.; Springer: Singapore, 2020; Volume 18, pp. 329–351.
28. Madurwar, M.V.; Ralegaonkar, R.V.; Mandavgane, S.A. Application of agro-waste for sustainable construction materials: A review. *Constr. Build. Mater.* **2013**, *38*, 872–878. [CrossRef]
29. Liuzzi, S.; Sanarica, S.; Stefanizzi, P. Use of agro-wastes in building materials in the Mediterranean area: A review. *Energy Procedia* **2017**, *126*, 242–249. [CrossRef]
30. Tawasil, D.N.B.; Aminudin, E.; Abdul Shukor Lim, N.H.; Nik Soh, N.M.Z.; Leng, P.C.; Ling, G.H.T.; Ahmad, M.H. Coconut fibre and sawdust as green building materials: A laboratory assessment on physical and mechanical properties of particleboards. *Buildings* **2021**, *11*, 256. [CrossRef]

31. Hebbar, K.B.; Abhin, P.S.; Jose, V.S.; Neethu, P.; Santhosh, A.; Shil, S.; Prasad, P.V.V. Predicting the Potential Suitable Climate for Coconut (*Cocos nucifera* L.) Cultivation in India under Climate Change Scenarios Using the MaxEnt Model. *Plants* **2022**, *11*, 731. [CrossRef]
32. Antwi-Boasiako, C.; Ofosuhene, L.; Boadu, K.B. Suitability of sawdust from three tropical timbers for wood-cement composites. *J. Sustain. For.* **2018**, *37*, 414–428. [CrossRef]
33. Mwango, A.; Kambole, C. Engineering characteristics and potential increased utilisation of sawdust composites in construction—A review. *J. Build. Constr. Plan. Res.* **2019**, *7*, 59–88. [CrossRef]
34. Wang, B.; Yan, L.; Kasal, B. A review of coir fibre and coir fibre reinforced cement-based composite materials (2000–2021). *J. Clean. Prod.* **2022**, *338*, 130676. [CrossRef]
35. Ahmad, J.; Majdi, A.; Al-Fakih, A.; Deifalla, A.F.; Althoey, F.; El Ouni, M.H.; El-Shorbagy, M.A. Mechanical and Durability Performance of Coconut Fiber Reinforced Concrete: A State-of-the-Art Review. *Materials* **2022**, *15*, 3601. [CrossRef]
36. Khedari, J.; Watsanasathaporn, P.; Hirunlabh, J. Development of fibre-based soil–cement block with low thermal conductivity. *Cem. Concr. Compos.* **2005**, *27*, 111–116. [CrossRef]
37. Thanushan, K.; Yogananth, Y.; Sangeeth, P.; Coonghe, J.G.; Sathiparan, N. Strength and Durability Characteristics of Coconut Fibre Reinforced Earth Cement Blocks. *J. Nat. Fibers* **2021**, *18*, 773–788. [CrossRef]
38. Thanushan, K.; Sathiparan, N. Mechanical performance and durability of banana fibre and coconut coir reinforced cement stabilized soil blocks. *Materialia* **2022**, *21*, 101309. [CrossRef]
39. Danso, H.; Martinson, B.; Ali, M.; Mant, C. Performance characteristics of enhanced soil blocks: A quantitative review. *Build. Res. Inf.* **2015**, *43*, 253–262. [CrossRef]
40. Sangma, S.; Pohti, L.; Tripura, D.D. Size Effect of Fiber on Mechanical Properties of Mud Earth Blocks. In *Recycled Waste Materials*; Agnihotri, A.K., Reddy, K.R., Bansal, A., Eds.; Springer: Berlin/Heidelberg, Germany, 2019; pp. 119–125.
41. Purnomo, H.; Arini, S.W. Experimental Evaluation of Three Different Humidity Conditions to Physical and Mechanical Properties of Three Different Mixtures of Unfired Soil Bricks. *Makara J. Technol.* **2019**, *23*, 92–102. [CrossRef]
42. Demir, I. Effect of organic residues addition on the technological properties of clay bricks. *Waste Manag.* **2008**, *28*, 622–627. [CrossRef]
43. Ouattara, S.; Boffoue, M.O.; Assande, A.A.; Kouadio, K.C.; Kouakou, C.H.; Emeruwa, E.; Pasres. Use of Vegetable Fibers as Reinforcement in the Structure of Compressed Ground Bricks: Influence of Sawdust on the Rheological Properties of Compressed Clay Brick. *Am. J. Mater. Sci. Eng.* **2016**, *4*, 13–19.
44. Vilane, B.R.T. Assessment of stabilisation of adobes by confined compression tests. *Biosyst. Eng.* **2010**, *106*, 551–558. [CrossRef]
45. Jokhio, G.A.; Mohsin, S.M.S.; Gul, Y. Two-fold sustainability-Adobe with sawdust as partial sand replacement. *IOP Conf. Ser. Mater. Sci. Eng.* **2018**, *342*, 012069. [CrossRef]
46. Ganga, G.; Nsongo, T.; Elenga, H.; Mabiala, B.; Tatsiete, T.T. Effect of incorporation of chips and wood dust mahogany on mechanical and acoustic behavior of brick clay. *J. Build. Constr. Plan. Res.* **2014**, *2*, 198–208.
47. Tatane, M.; Akhzouz, H.; Elminor, H.; Feddaoui, M.B. Thermal, Mechanical and Physical Behavior of Compressed Earth Blocks Loads by Natural Wastes. *Int. J. Civ. Eng. Technol.* **2018**, *9*, 1353–1368.
48. De Castrillo, M.C.; Ioannou, I.; Philokyprou, M. Reproduction of traditional adobes using varying percentage contents of straw and sawdust. *Constr. Build. Mater.* **2021**, *294*, 123516. [CrossRef]
49. Charai, M.; Sghiouri, H.; Mezrhab, A.; Karkri, M.; Elhammouti, K.; Nasri, H. Thermal performance and characterization of a sawdust-clay composite material. *Procedia Manuf.* **2020**, *46*, 690–697. [CrossRef]
50. Udawattha, C.; Halwatura, R. Thermal performance and structural cooling analysis of brick, cement block, and mud concrete block. *Adv. Build. Energy Res.* **2016**, *12*, 150–163. [CrossRef]
51. *ASTM D698*; Standard Test Methods for Laboratory Compaction Characteristics of Soil Using Standard Effort (12,400 ft-lbf/ft^3 (600 kN-m/m^3)). ASTM International: West Conshohocken, PA, USA, 2012.
52. *BS 1377-2*; Methods of Test for Soils for Civil Engineering Purposes, Part 2: Classification Tests. British Standards Institution: London, UK, 1990.
53. *BS EN 771-1*; Specification for Masonry Units. Part 1: Clay Masonry Units. British Standards Institution: London, UK, 2003.
54. Vosteen, H.D.; Schellschmidt, R. Influence of temperature on thermal conductivity, thermal capacity and thermal diffusivity for different types of rock. *Phys. Chem. Earth Parts A/B/C* **2003**, *28*, 499–509. [CrossRef]
55. *BS EN ISO 6946*; Building Components and Building Elements—Thermal Resistance and Thermal Transmittance—Calculation methods. British Standards Institution: London, UK, 2017.
56. Gaspar, K.; Casals, M.; Gangolells, M. A comparison of standardized calculation methods for in situ measurements of façades U-value. *Energy Build.* **2016**, *130*, 592–599. [CrossRef]
57. Gaspar, K.; Casals, M.; Gangolells, M. Review of criteria for determining HFM minimum test duration. *Energy Build.* **2018**, *176*, 360–370. [CrossRef]
58. Choi, D.S.; Ko, M.J. Analysis of Convergence Characteristics of Average Method Regulated by ISO 9869-1 for Evaluating In Situ Thermal Resistance and Thermal Transmittance of Opaque Exterior Walls. *Energies* **2019**, *12*, 1989. [CrossRef]
59. *BS ISO 9869-1*; Thermal Insulation—Building Elements—In-Situ Measurement of Thermal Resistance and Thermal Transmittance—Part 1: Heat Flow Meter Method. British Standards Institution: London, UK, 2014.

60. Gaspar, K.; Casals, M.; Gangolells, M. In situ measurement of façades with a low U-value: Avoiding deviations. *Energy Build.* **2018**, *170*, 61–73. [CrossRef]
61. Soares, N.; Martins, C.; Gonçalves, M.; Santos, P.; Da Silva, L.S.; Costa, J.J. Laboratory and in-situ non-destructive methods to evaluate the thermal transmittance and behavior of walls, windows, and construction elements with innovative materials: A review. *Energy Build.* **2019**, *182*, 88–110. [CrossRef]
62. Zhao, X.; Mofid, S.A.; Al Hulayel, M.R.; Saxe, G.W.; Jelle, B.P.; Yang, R. Reduced-scale hot box method for thermal characterization of window insulation materials. *Appl. Therm. Eng.* **2019**, *160*, 114026. [CrossRef]
63. Asdrubali, F.; Baldinelli, G. Thermal transmittance measurements with the hot box method: Calibration, experimental procedures, and uncertainty analyses of three different approaches. *Energy Build.* **2011**, *43*, 1618–1626. [CrossRef]
64. Lu, X.; Memari, A.M. Comparative study of Hot Box Test Method using laboratory evaluation of thermal properties of a given building envelope system type. *Energy Build.* **2018**, *178*, 130–139. [CrossRef]
65. Lu, X.; Memari, A.M. Comparison of the Experimental Measurement Methods for Building Envelope Thermal Transmittance. *Buildings* **2022**, *12*, 282. [CrossRef]
66. Buratti, C.; Belloni, E.; Lunghi, L.; Borri, A.; Castori, G.; Corradi, M. Mechanical characterization and thermal conductivity measurements using of a new 'small hot-box' apparatus: Innovative insulating reinforced coatings analysis. *J. Build. Eng.* **2016**, *7*, 63–70. [CrossRef]
67. Meng, X.; Luo, T.; Gao, Y.; Zhang, L.; Shen, Q.; Long, E. A new simple method to measure wall thermal transmittance in situ and its adaptability analysis. *Appl. Therm. Eng.* **2017**, *122*, 747–757. [CrossRef]
68. Laborel-Préneron, A.; Magniont, C.; Aubert, J.E. Hygrothermal properties of unfired earth bricks: Effect of barley straw, hemp shiv and corn cob addition. *Energy Build.* **2018**, *178*, 265–278. [CrossRef]
69. Laborel-Preneron, A.; Aubert, J.E.; Magniont, C.; Tribout, C.; Bertron, A. Plant aggregates and fibers in earth construction materials: A review. *Constr. Build. Mater.* **2016**, *111*, 719–734. [CrossRef]
70. Jannat, N.; Hussien, A.; Abdullah, B.; Cotgrave, A. Application of agro and non-agro waste materials for unfired earth blocks construction: A review. *Constr. Build. Mater.* **2020**, *254*, 119346. [CrossRef]
71. Jannat, N.; Al-Mufti, R.L.; Hussien, A.; Abdullah, B.; Cotgrave, A. Influences of agro-wastes on the physico-mechanical and durability properties of unfired clay blocks. *Constr. Build. Mater.* **2022**, *318*, 126011. [CrossRef]
72. Babé, C.; Kidmo, D.K.; Tom, A.; Mvondo, R.R.N.; Kola, B.; Djongyang, N. Effect of neem (*Azadirachta Indica*) fibers on mechanical, thermal and durability properties of adobe bricks. *Energy Rep.* **2021**, *7*, 686–698. [CrossRef]
73. Kazmi, S.M.S.; Munir, M.J.; Patnaikuni, I.; Wu, Y.F.; Fawad, U. Thermal performance enhancement of eco-friendly bricks incorporating agro-wastes. *Energy Build.* **2018**, *158*, 1117–1129. [CrossRef]
74. Tornay, N.; Schoetter, R.; Bonhomme, M.; Faraut, S.; Masson, V. GENIUS: A methodology to define a detailed description of buildings for urban climate and building energy consumption simulations. *Urban Clim.* **2017**, *20*, 75–93. [CrossRef]
75. Stapulionienė, R.; Vaitkus, S.; Vėjelis, S.; Sankauskaitė, A. Investigation of thermal conductivity of natural fibres processed by different mechanical methods. *Int. J. Precis. Eng. Manuf.* **2016**, *17*, 1371–1381. [CrossRef]
76. Pásztory, Z. An overview of factors influencing thermal conductivity of building insulation materials. *J. Build. Eng.* **2021**, *44*, 102604.
77. Ouedraogo, M.; Dao, K.; Millogo, Y.; Aubert, J.E.; Messan, A.; Seynou, M.; Zerbo, L.; Gomina, M. Physical, thermal and mechanical properties of adobes stabilized with fonio (*Digitaria exilis*) straw. *J. Build. Eng.* **2019**, *23*, 250–258. [CrossRef]
78. Raut, A.N.; Gomez, C.P. Development of thermally efficient fibre-based eco-friendly brick reusing locally available waste materials. *Constr. Build. Mater.* **2017**, *133*, 275–284. [CrossRef]
79. Zhang, L.; Yang, L.; Jelle, B.P.; Wang, Y.; Gustavsen, A. Hygrothermal properties of compressed earthen bricks. *Constr. Build. Mater.* **2018**, *162*, 576–583. [CrossRef]
80. Kandula, R.; Sanaka, S.P.; Prasad, A.V.R.; Reddy, K.H. Thermo-physical and Fire Properties of Natural Fiber Composites for Energy Saving Applications. *J. Nat. Fibers* **2022**, 1–13. [CrossRef]
81. Babé, C.; Kidmo, D.K.; Tom, A.; Mvondo, R.R.N.; Boum, R.B.E.; Djongyang, N. Thermomechanical characterization and durability of adobes reinforced with millet waste fibers (sorghum bicolor). *Case Stud. Constr. Mater.* **2020**, *13*, e00422. [CrossRef]
82. Millogo, Y.; Morel, J.C.; Aubert, J.E.; Ghavami, K. Experimental analysis of Pressed Adobe Blocks reinforced with *Hibiscus cannabinus* fibers. *Constr. Build. Mater.* **2014**, *52*, 71–78. [CrossRef]
83. Khoudja, D.; Taallah, B.; Izemmouren, O.; Aggoun, S.; Herihiri, O.; Guettala, A. Mechanical and thermophysical properties of raw earth bricks incorporating date palm waste. *Constr. Build. Mater.* **2021**, *270*, 121824. [CrossRef]
84. Zeghari, K.; Gounni, A.; Louahlia, H.; Marion, M.; Boutouil, M.; Goodhew, S.; Streif, F. Novel Dual Walling Cob Building: Dynamic Thermal Performance. *Energies* **2021**, *14*, 7663. [CrossRef]
85. Medjelekh, D.; Ulmet, L.; Abdou, S.; Dubois, F. A field study of thermal and hygric inertia and its effects on indoor thermal comfort: Characterization of travertine stone envelope. *Build. Environ.* **2016**, *106*, 57–77. [CrossRef]
86. Lizana, J.; Chacartegui, R.; Barrios-Padura, A.; Valverde, J.M. Advances in thermal energy storage materials and their applications towards zero energy buildings: A critical review. *Appl. Energy* **2017**, *203*, 219–239. [CrossRef]
87. Jeanjean, A.; Olives, R.; Py, X. Selection criteria of thermal mass materials for low-energy building construction applied to conventional and alternative materials. *Energy Build.* **2013**, *63*, 36–48. [CrossRef]

88. Atiki, E.; Taallah, B.; Feia, S.; Almeasar, K.S.; Guettala, A. Effects of Incorporating Date Palm Waste as a Thermal Insulating Material on the Physical Properties and Mechanical Behavior of Compressed Earth Block. *J. Nat. Fibers* **2021**, 1–18. [CrossRef]
89. Bruno, A.W.; Gallipoli, D.; Perlot, C.; Kallel, H. Thermal performance of fired and unfired earth bricks walls. *J. Build. Eng.* **2020**, *28*, 101017. [CrossRef]
90. Ojerinde, A. The Use of Rice Husk Ash (RHA) as Stabilizer in Compressed Earth Block (CEB) for Affordable Houses. Ph.D Thesis, Cardiff University, Cardiff, UK, 2020.
91. Krstić, H.; Miličević, I.; Markulak, D.; Domazetović, M. Thermal Performance Assessment of a Wall Made of Lightweight Concrete Blocks with Recycled Brick and Ground Polystyrene. *Buildings* **2021**, *11*, 584. [CrossRef]
92. Chowdhury, D.; Neogi, S. Thermal performance evaluation of traditional walls and roof used in tropical climate using guarded hot box. *Constr. Build. Mater.* **2019**, *218*, 73–89. [CrossRef]
93. Callejas, I.J.A.; Durante, L.C.; de Oliveira, A.S. Thermal resistance and conductivity of recycled construction and demolition waste (RCDW) concrete blocks. *REM Int. Eng. J.* **2017**, *70*, 167–173. [CrossRef]
94. Teixeira, E.R.; Machado, G.; de P. Junior, A.; Guarnier, C.; Fernandes, J.; Silva, S.M.; Mateus, R. Mechanical and thermal performance characterisation of compressed earth blocks. *Energies* **2020**, *13*, 2978. [CrossRef]
95. Douzane, O.; Promis, G.; Roucoult, J.M.; Le, A.D.T.; Langlet, T. Hygrothermal performance of a straw bale building: In situ and laboratory investigations. *J. Build. Eng.* **2016**, *8*, 91–98. [CrossRef]